Corrosion Science 111 (2016) 846–849

Contents lists available at ScienceDirect

Corrosion Science

journal homepage: www.elsevier.com/locate/corsci

Short communication

A novel approach to exploring glassy alloys with high oxidation resistance in the supercooled liquid region

Ka Ram Lim[a,*,1], Tae Hee Cho[b,1], Sung Hyun Park[b], Min Young Na[b], Kang Cheol Kim[b], Young Sang Na[a], Won Tae Kim[c], Do Hyang Kim[b,*]

[a] Metallic Materials Division, Korea Institute of Materials Science, 797 Changwondaero, Seongsan-gu, Changwon, Gyeongnam 642-831, South Korea
[b] Center for Non-crystalline Materials, Department of Materials Science and Engineering, Yonsei University, 134 Shinchon-dong, Seodaemun-gu, Seoul 120-749, South Korea
[c] Department of Optical Engineering, Cheongju University, 36 Naedock-dong, Cheongju 360-764, South Korea

ARTICLE INFO

Article history:
Received 21 March 2016
Received in revised form 14 April 2016
Accepted 1 May 2016
Available online 4 May 2016

Keywords:
A. Alloy
B. TEM
C. Amorphous structures
C. Oxidation
C. Passive Films

ABSTRACT

In the present study, we propose a novel approach to exploring glassy alloys with high oxidation resistance in their supercooled liquid region. The oxidation resistance of the Zr-based metallic glasses can be strongly enhanced when the glassy surface is covered by a native amorphous metal oxide film. We have investigated the effect of codoping Al and Ti into the amorphous zirconia on glass stability of the amorphous oxide by selecting $Ni_{45}Zr_{35-x}Ti_{20}Al_x$ quaternary metallic glass system. The thermogravimetric analysis suggests that codoping multi-components is an effective way to enhance the glass stability of the amorphous oxide film.

There have been various efforts to use metallic glasses for structural or functional applications [1–9]. However, the oxidation can be a main problem when the fabrication processes are conducted in the supercooled liquid (SCL) state [4–9]. For example, the oxidation results in a reduction of gloss on glassy surface [10], which is undesirable for the structural applications. In addition, poor oxidation resistance of atomized metallic glass powders may disrupt consolidation, since the surface oxides hinder interfacial bonding between the powders [11–13]. Previous studies on the oxidation behavior of metallic glasses suggested that drastic oxidation can occur above the glass transition temperature (T_g) [14–21]. The rapid oxidation in the SCL region can be attributed to strong viscosity drop above the T_g [7,22,23] and high oxygen permeability of the oxide film [18–21]. Hence, metallic glasses with higher oxidation resistance in their SCL region are more favorable for the forming processes under air atmosphere.

According to previous studies [18–21], an oxide film on the metallic glass plays a key role in determining the oxidation rate in the SCL region. Amorphous metal oxide films are observed at initial stages of oxidation in metallic glasses [19–21,24], and they provides effective resistance against oxidation. The atomic structure of the oxide film strongly depends on its chemical composition, which is closely linked to that of the substrate. The alloying elements with high oxygen affinity preferentially participate in oxidation reaction, and form homogeneous amorphous mixture at initial stages of surface oxide formation, since all the alloying elements are randomly distributed in the substrate. Therefore, for the metallic glasses, the chemical composition of the initial oxide film can be easily tailored by controlling the alloy composition. In the case of Zr-based metallic glasses, it has been reported that the amorphous metal oxide film can be strongly stabilized by adding an alloying element such as beryllium (Be), since Be has a high oxygen affinity but very limited solubility in crystalline zirconia [24,25]. The high oxygen affinity is required for the alloying element to participate in the oxidation reaction, and once the alloying element dissolves into the amorphous oxide, it suppresses amorphous-to-crystalline phase transformation by destabilizing the crystalline phase [24].

However, using Be as a stabilizer of the amorphous zirconia is not recommended, since Be is toxic and expensive. Instead, aluminum (Al) and titanium (Ti) can be good alternatives for stabilizing amorphous zirconia. Based on our previous researches [20,21], Al- and Ti-doped zirconia were observed to retain amorphous structure near the T_g of the substrate, indicating that both Al and Ti

* Corresponding authors.
E-mail addresses: krlim@kims.re.kr (K.R. Lim), dohkim@yonsei.ac.kr (D.H. Kim).
[1] These authors contributed equally to this work.

http://dx.doi.org/10.1016/j.corsci.2016.05.001
0010-938X/

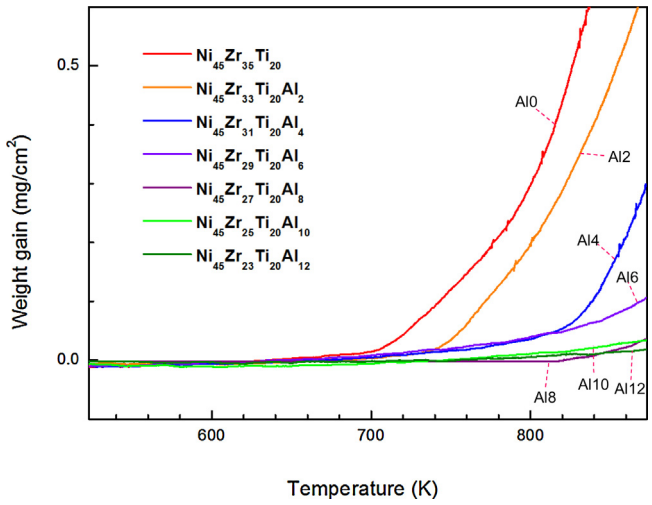

Fig. 1. Temperature–weight gain plots obtained from as-melt-spun $Ni_{45}Zr_{35-x}Ti_{20}Al_x$ (x = 0, 2, 4, 6, 8, 10, and 12) ribbons during continuous heating up to 873 K with a heating rate of 40 K/min.

work in stabilizing the amorphous zirconia. Unfortunately, however, adding only one dopant between Al and Ti seems not to have a potent effect in stabilizing the amorphous state, since each of them has a small amount of solubility in crystalline zirconia [26,27] unlike Be, which allows the local crystallization within the Al- or Ti-doped amorphous zirconia film in the supercooled liquid region [20,21]. So we selected $Ni_{45}Zr_{35-x}Ti_{20}Al_x$ quaternary metallic glass system, which has three components with high oxygen affinity (Zr, Ti, and Al) [25], since we expected that codoping Al and Ti into the amorphous zirconia can be an effective way to enhance the glass stability of the amorphous zirconia.

Alloys of nominal composition $Ni_{45}Zr_{35-x}Ti_{20}Al_x$ (x = 0, 2, 4, 6, 8, 10, and 12) were prepared by arc-melting pure (>99.9 at.%) metals under an argon atmosphere. Rapidly solidified amorphous ribbons with a width of ~5 mm and a thickness of ~50 μm were produced by melt-spinning method under an argon atmosphere. The thermal analysis of as-melt-spun ribbons was studied using differential scanning calorimetry (DSC, Perkin Elmer DSC 7) at a heating rate of 40 K/min. Oxidation behavior of the ribbons was studied under the condition of short-term air exposure using thermogravimetric analyzer (TGA, Perkin Elmer TGA 4000). The specimens were continuously heated up to 873 K with a heating rate of 40 K/min, and the net flow rate of high-purity (>99.99%) dry air was kept constant at 20 cm^3/min. The change in the surface structure for the glassy ribbons upon oxidation was examined by transmission electron microscopy (TEM, JEOL 2100F) equipped with an energy dispersive spectrometer (EDS, Oxford Instruments INCA x-act 51-ADD0069). Cross-sectional thin foil specimens for TEM analysis were prepared by focused ion beam milling (Dual-beam FIB, FEI Helios NanoLab).

Fig. 1 shows temperature–weight gain plots obtained from the thermo-gravimetric analysis, and thermal properties of the as-melt-spun ribbons measured by DSC are presented in Table 1. As shown in Fig. 1, it is observed that oxidation rate is gradually reduced as Al content increases. The results indicate that the addition of Al not only extends the SCL region (ΔT_x) (see Table 1), but also enhances the oxidation resistance. The alloys with Al content of 2 at.% or less show poor oxidation resistance in the SCL region, while the alloys with Al content of 4 at.% or more are rarely oxidized in their SCL region. In the case of the lower Al-content alloys, the oxidation rate abruptly increases near their glass transition temperatures. The results suggest that Al content is closely associated with the characteristics of the oxide film. To investigate the role of the oxide film (with or without Al) in the oxidation kinetics of the

Table 1
Thermal properties of as-melt-spun $Ni_{45}Zr_{35-x}Ti_{20}Al_x$ (x = 0, 2, 4, 6, 8, 10, and 12) ribbons (heating rate: 40 K/min): glass transition temperature T_g, crystallization onset temperature T_x, supercooled liquid region ΔT_x ($\Delta T_x = T_x - T_g$).

Alloys (at.%)	T_g (K)	T_x (K)	ΔT_x (K)
$Ni_{45}Zr_{35}Ti_{20}$	725	753	28
$Ni_{45}Zr_{33}Ti_{20}Al_2$	740	773	33
$Ni_{45}Zr_{31}Ti_{20}Al_4$	743	786	43
$Ni_{45}Zr_{29}Ti_{20}Al_6$	745	795	50
$Ni_{45}Zr_{27}Ti_{20}Al_8$	764	807	43
$Ni_{45}Zr_{25}Ti_{20}Al_{10}$	779	826	47
$Ni_{45}Zr_{23}Ti_{20}Al_{12}$	784	839	55

glassy alloys, we focused on the initial oxidation stages in the SCL region.

Fig. 2a and b exhibits temperature–weight gain plots obtained from the thermo-gravimetric analysis of as-melt-spun $Ni_{45}Zr_{35}Ti_{20}$ and $Ni_{45}Zr_{31}Ti_{20}Al_4$ ribbons which are superimposed on their DSC curves. As shown in these figures, the addition of Al into the Ni-Zr-Ti alloy resulted in a quite different oxidation behavior in the SCL region: the $Ni_{45}Zr_{35}Ti_{20}$ ribbon begins to rapidly oxidize near the T_g, while the $Ni_{45}Zr_{31}Ti_{20}Al_4$ ribbon maintains the low oxidation rate in the SCL region. To investigate the reason for such a big difference in the oxidation behavior depending on Al content, the samples were heated up to near their T_g, i.e. 722 K (3 K below T_g) for $Ni_{45}Zr_{35}Ti_{20}$ and 743 K (T_g) for $Ni_{45}Zr_{31}Ti_{20}Al_4$ with a heating rate of 40 K/min, and then the cross-sectional microstructures of the samples were carefully examined using TEM.

Cross-sectional bright-field TEM images in Fig. 3a and b show the oxide film and the substrate obtained from $Ni_{45}Zr_{35}Ti_{20}$ and $Ni_{45}Zr_{31}Ti_{20}Al_4$ ribbons after continuous heating up to 722 K and 743 K, respectively. In the case of $Ni_{45}Zr_{35}Ti_{20}$, fan-shaped oxide islands grown into the amorphous matrix are observed underneath the oxide film, since oxygen ions can be easily flowed mainly through the crystallized region. However, in the case of $Ni_{45}Zr_{31}Ti_{20}Al_4$, there is no dendritic growth underneath the oxide film. Fig. 3c and d shows the magnified High resolution TEM (HRTEM) images obtained from the regions marked by the dashed line in Fig. 3a and b, respectively. The insets of Fig. 3c and d exhibit the fast Fourier transform (FFT) patterns obtained from the HRTEM images. In Fig. 3c, it is found that the oxide film on the $Ni_{45}Zr_{35}Ti_{20}$ alloy has amorphous structure but it is partially crystallized. In particular, the crystallized regions in the oxide film are connected to the fan-shaped oxide islands, indicating that the crystalline oxide has highly increased oxygen permeability compared to the amorphous oxide. In this case, the oxygen ions can be rapidly transported from the surface of the crystallized regions within the oxide layer to the amorphous matrix. Therefore, in this case, the atomic structure of the oxide film is considered to have a decisive effect on the oxidation rate in the SCL region. Whereas the oxide film on the $Ni_{45}Zr_{31}Ti_{20}Al_4$ alloy still retains fully amorphous structure. From the results, we confirmed that Al plays an important role in enhancing the thermal stability of the amorphous oxide film, which effectively protects the substrate in SCL state against oxidation. Here, there can be two important questions. One is why the rapid oxidation occurs only through the crystallized regions within the oxide film, the other is how the addition of Al strongly can enhance the thermal stability of the amorphous oxide film.

To answer those questions, the chemical composition of each oxide film was measured by TEM-EDS analysis (inserted in Fig. 3a and b). Firstly, in the case of $Ni_{45}Zr_{35}Ti_{20}$, the chemical composition of the oxide film is around $Zr_{24}Ti_{12}O_{64}$ (unknown phase), and there is no difference in chemical composition between the crystalline and the amorphous oxides. It is known that amorphous oxides do not provide fast ion diffusion paths such as grain boundaries